Reducing Grid Dependency and Emissions: Optimizing Renewable Energy Forecasts for Data Centers

Sarika de Bruyn, Sed2194

May 11, 2025

1 Introduction

The rapid expansion of digital infrastructure, particularly data centers, has highlighted the urgent need to address their significant energy demands and associated carbon emissions. Data centers, which are integral to modern computing and cloud services, are now major energy consumers, driving a critical need for sustainable and cost-effective energy solutions. [1] Renewable energy sources, primarily solar and wind, offer promising pathways toward reducing carbon footprints. However, their inherent intermittency poses operational challenges, especially in contexts that require uninterrupted power supply. [2]

Accurate forecasting of renewable energy availability emerges as a pivotal strategy for optimizing renewable-powered data centers, minimizing reliance on expensive and carbon-intensive grid electricity. However, the misalignment between the forecast and actual renewable energy generation can lead to increased operational costs and higher carbon emissions due to the use of the grid fallback.[3]

In this study, I explore the relationship between the quality and uncertainty of machine learning-driven renewable energy forecasts and the operational effectiveness of solar- and wind-powered data centers. By evaluating advanced forecasting models, specifically NGBoost and TabPFN, against traditional baselines (Perfect-Foresight and Climatology Models), I quantify how predictive accuracy impacts key performance metrics, including grid fallback frequency, emissions, and operational costs. The locations chosen for this study—Yuma, Arizona, for solar energy and Mount Storm, West Virginia, for wind energy—provide ideal conditions where the renewable energy source is plentiful, consistent, and well-documented.[4] [5]

In addition, I integrate a battery energy storage system (BESS) to store surplus renewable energy when supply exceeds demand and to discharge stored energy when supply is insufficient, reducing grid fallback and mitigating operational disruptions. Through rigorous scenario analyses, my objective is to provide clear insight into how improved forecasting capabilities can enhance the economic viability and sustainability of renewable energy data centers, guiding future investments and operational strategies in green computing infrastructure.

2 Methodology

This study quantifies how hour-ahead solar and wind forecasts affect a 40MW, renewably powered data-centre's operations. The models employed in this study are NGBoost and TabPFN, which are benchmarked against climatology and an oracle "perfect-foresight" upper bound. The

[1] **Uptime Institute.** *Global Data Center Survey 2024.* Uptime Intelligence Report, 2024, uptimeinstitute.com.

[2] **E3.** *Load Growth Is Here to Stay, but Are Data Centers?* E3 White Paper, 2024, ethree.com.

[3] **ASCEE.** *International Journal of Research in Community Services (IJRCS).* ASCEE, 2025, pubs2.ascee.org.

[4] **National Climatic Data Center.** *Sunniest U.S. Cities.* National Oceanic and Atmospheric Administration, 2024, ncei.noaa.gov.

[5] **Dominion Energy.** *Mount Storm Wind Farm Fact Sheet.* Dominion Energy, 2024, dominionenergy.com.

forecasting pipeline combines statistical learning with domain physics via irradiance-to-power and wind-to-power equations, enabling direct comparison on grid fallback, cost, and emissions.

This study assumes a hypothetical data center and renewable energy infrastructure, modeled based on realistic parameters derived from comparable facilities. The data center is assumed to have a peak power demand of 40 MW, consistent with the requirements of a large-scale computational facility. The solar farm, designed as a utility-scale installation, also has a capacity of 40 MW, consisting of approximately 160,000 solar panels. Each panel has an area of 1.6 m^2, resulting in a total panel area of 256,000 m^2. The efficiency of the panels is set at 20%, and the system's performance ratio is 0.8. [6][7]Additionally, the wind farm is assumed to have a capacity of 40 MW, comprising 16 turbines, each rated at 2.5 MW, with a rotor diameter of 100 meters and a hub height of 80 meters. The turbine efficiency is assumed to be 40%, and the air density is considered to be 1.121 kg/m^3.[8][9]

2.1 Data Collection and Preprocessing

Solar data was obtained from the National Solar Radiation Database (NSRDB), covering Yuma, Arizona, from 2018 to 2023.[10] Wind data was gathered from the WindExchange portal, focusing on Mount Storm, West Virginia, for the same period.[11] The solar dataset includes variables such as Global Horizontal Irradiance (GHI), Direct Normal Irradiance (DNI), Diffuse Horizontal Irradiance (DHI), temperature, wind speed, relative humidity, atmospheric pressure, ozone, dew point, and cloud type. The wind dataset includes wind speed, temperature, atmospheric pressure, relative humidity, and dew point.

Missing data were treated in two steps: gaps of $\leq 3\,\mathrm{h}$ were linearly interpolated to maintain temporal continuity, whereas longer gaps were removed to avoid distortion. The cleaned records were then saved as year-tagged CSV files (e.g., `solar_YYYY.csv`, `wind_YYYY.csv`).

2.2 Model Development

2.2.1 Baseline Models

The Climatology Model uses historical hourly averages from 2018 to 2022 to predict GHI (W/m^2) and wind speed (m/s) for 2023. This model serves as a basic reference to evaluate the improvements offered by advanced machine learning techniques. The Perfect-Foresight Model uses actual forecast results from 2023 and serves as an ideal benchmark, representing the maximum potential performance if forecasts were entirely accurate. These models were then converted into solar- or wind- farm total output for 2023 using the following equations:

Equation 1: Solar Power Conversion Equation [12]

$$\text{Power (MW)} = \frac{\text{GHI} \times \cos(\text{zenith angle}) \times \text{PANEL\_AREA} \times \text{EFFICIENCY} \times \text{PERF\_RATIO}}{10^6}$$

Where the zenith angle is calculated as:

$$\text{zenith angle} = \left(\frac{|12 - \text{hour}|}{12} \right) \times 90^\circ$$

[6]**Solar Energy Industries Association (SEIA).** *Utility-Scale Solar Power Overview.* Solar Energy Industries Association, seia.org.

[7]**First Solar.** *Utility-Scale PV Power Plants.* First Solar, firstsolar.com.

[8]**National Renewable Energy Laboratory (NREL).** *Land-Use Requirements for Wind Turbines.* U.S. Department of Energy, nrel.gov.

[9]**Vestas.** *V100-2.0 MW Specs.* GE Renewable Energy Turbines, vestas.com.

[10]**National Renewable Energy Laboratory (NREL).** *National Solar Radiation Data Base (NSRDB).* U.S. Department of Energy, 2021, nsrdb.nrel.gov

[11]**National Renewable Energy Laboratory (NREL).** *WIND Toolkit Data Set, Hub-Height 100 m Layer.* U.S. Department of Energy, windexchange.energy.gov.

[12]**Maysun Solar.** *Performance Ratio: Do You Know How to Calculate It?* Maysun Solar Blog, maysunsolar.com.

Equation 2: Wind Power Conversion Equation [13]

$$\text{Power (MW)} = \frac{0.5 \times \text{AIR\_DENSITY} \times \text{SWEEP\_AREA} \times \text{EFFICIENCY} \times \text{TURBINE\_COUNT} \times (\text{Wind Speed})^3}{1{,}000{,}000}$$

2.2.2 Common Workflow for NGBoost and TabPFN Models

All models draw on the same CSV files.For each timestamp, the table records cyclic encodings of the hour of day and the day of year (sine–cosine pairs), a binary holiday flag, the full meteorological state where relevant, five lags of the target variable at $1, 3, 6, 24$ and 168 hours, and the 24-hour rolling mean and standard deviation of that target.

Because photovoltaic output varies with both sun angle and panel temperature, the solar feature set also holds the pvlib-derived zenith angle and a temperature-derating factor:

$$\text{eff}_{\text{temp}} \;=\; 1 \;-\; \gamma\,\big(T \;-\; 25^{\circ}\text{C}\big)$$

where T is ambient temperature, $\gamma = 0.0045\ \text{C}^{-1}$ is the module temperature coefficient. Categorical variables such as cloud type are one-hot encoded, although ideally this should be done using ordinal encoding to better represent the natural progression of cloud coverage. When a model predicts GHI or wind speed, those values are converted to electrical power using either **Equation 1** or **Equation 2** so that every forecast ultimately appears as MW on a consistent hourly grid; the resulting power series are archived at both hourly and monthly resolution for 2023.

2.2.3 NGBoost Models

NGBoost fits separate models to the solar and wind sites but keeps the same optimisation protocol for both. It trains gradient-boosted decision trees with a Normal likelihood; fifteen Optuna trials select the learning rate, maximum tree depth, and ensemble size. The algorithm returns a predictive mean and variance, which are later sampled in the Monte-Carlo uncertainty analysis.

For the solar site NGBoost is asked to predict the residual between the observed global horizontal irradiance (GHI) and the five-year monthly-hourly climatological mean. This residual-learning approach directs the booster to concentrate on short-term departures caused by transient clouds rather than re-learning the long-term solar cycle that the climatology already captures. The efficiency-derating term `eff_temp` and the zenith angle appear as ordinary predictors alongside the meteorological drivers and lagged GHI values.

For the wind site NGBoost predicts the wind-speed magnitude itself. Preliminary experiments showed that residual learning offered no accuracy benefit once the cubic wind-power conversion was applied, so the model focuses on capturing the full variability of wind speed from meteorological context and short-range lags.

2.2.4 TabPFN Models

TabPFN employs a pre-trained transformer that adapts automatically to tabular data, requiring no manual hyper-parameter tuning. Training is executed on a GPU-enabled GoogleColab instance, reducing fit time from hours to minutes. Owing to its self-attention architecture, TabPFN can internalise temporal patterns that would otherwise need explicit sequence models.

For the solar site TabPFN mirrors NGBoost's residual-learning strategy. The model outputs the deviation from the climatological GHI baseline; that residual is added back to reconstruct GHI, which is then passed through **Equation 1**. All solar-specific predictors, including `eff_temp` and the zenith angle, are available to the transformer alongside the generic feature set.

For the wind site TabPFN converges on direct power prediction rather than wind speed. Validation results show that forecasting power in kilowatts and then scaling to megawatts yields a

[13] **Penn State EMSC 297.** *Wind Energy and Power Calculations.* Pennsylvania State University, e-education.psu.edu.

lower root-mean-square error than predicting speed first and applying the cubic law. The feature inputs remain identical to those of the wind NGBoost model, but no residual transformation is applied.

2.3 Dispatch Logic and Simulation

Before any grid simulation, each forecast series $Y(t)$ is affinely calibrated to the hold-out year via

$$\hat{Y}(t) \;=\; a\,Y(t) + b,$$

where the coefficients a and b are chosen to minimize unmet load in the battery dispatch model when fitted on 2022 and then applied to 2023.

The dynamic demand load for the data center was modeled as[14]:

$$D(t) = (C + V_c \times h(t) \times d(t) \times s(t)) \times \epsilon(t)$$

Where C = Constant base load (18 MW), V_c = Variable capacity (10 MW), $h(t)$ = Hourly profile factor, $d(t)$ = Day-of-week adjustment, $s(t)$ = Seasonal adjustment, and $\epsilon(t) \sim N(1.0, 0.05)$

A simple greedy algorithm then meets demand in three stages—first on-site renewables, then a 40 MWh usable (50 MWh nameplate) battery operating between 10 % and 90 % state of charge at 92.5 % round-trip efficiency[1], and finally grid fallback if necessary. To quantify uncertainty, we draw 100 synthetic forecast trajectories per model by sampling each model's predictive distribution and run each trajectory through the dispatch loop, producing P5, P50, and P95 estimates of unmet load, curtailment, and CO emissions.

2.4 Performance Metrics

Model skill on the hold-out year is quantified by the root-mean-square error (RMSE) and mean signed error (bias) of the resource variable (GHI or wind speed). We additionally report the median grid fallback, curtailment, and emissions drawn from the Monte Carlo ensemble. During model development, hyper-parameters were tuned via an expanding-window cross-validation (TimeSeriesSplit) on 2018–2022, but all final metrics are evaluated on the 2023 hold-out.

2.5 Cost Distribution for Solar and Wind Forecasts

I translate grid fallback into costs using the formula[15]:

$$\text{Cost (USD)} = \text{Grid Fallback (MWh)} \times \text{Cost Factor (USD per MWh)}$$

with Cost Factor = 1,000 × GRID_COST_USD_KWH. For each forecasting method—Climatology, NGBoost, and TabPFN—we run 50 Monte Carlo simulations: Climatology repeats the same deterministic forecast, whereas NGBoost and TabPFN apply the affine calibration above and then perturb forecasts with Gaussian noise derived from their residual standard deviation. Each synthetic forecast is dispatched greedily, and the resulting cost outcomes are displayed as box plots showing median, interquartile range, and overall spread

3 Results

This section presents the outcomes of evaluating forecasting models (Climatology, NGBoost, and TabPFN) for solar- and wind- powered farms . The goal is to assess how forecast accuracy influences grid fallback, energy demand met, and cost variability. The analysis focuses on comparing model performance across key metrics: Root Mean Square Error (RMSE), Coefficient of Variation (CV), Grid Fallback (MWh), Percentage of Demand Met, and Cost Distribution (USD).

[14] **Joint Legislative Audit and Review Commission (JLARC).** *Virginia Data Center Study.* Commonwealth of Virginia, jlarc.virginia.gov

[15] **U.S. Energy Information Administration (EIA).** *Wholesale Electricity Markets.* U.S. Department of Energy, eia.gov.

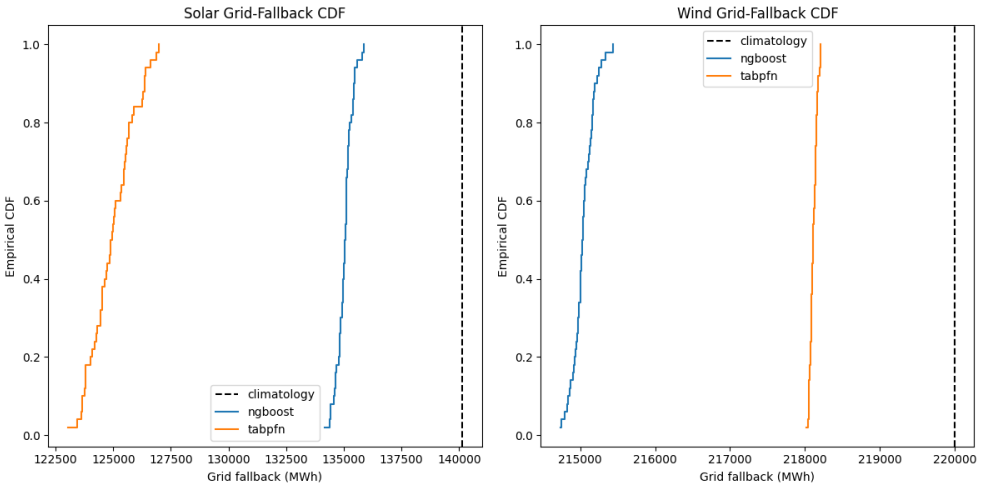

Figure 2: Cumulative Distribution Function (CDF) of Grid Fallback for Solar and Wind

3.1 Evaluation of Forecasting Models

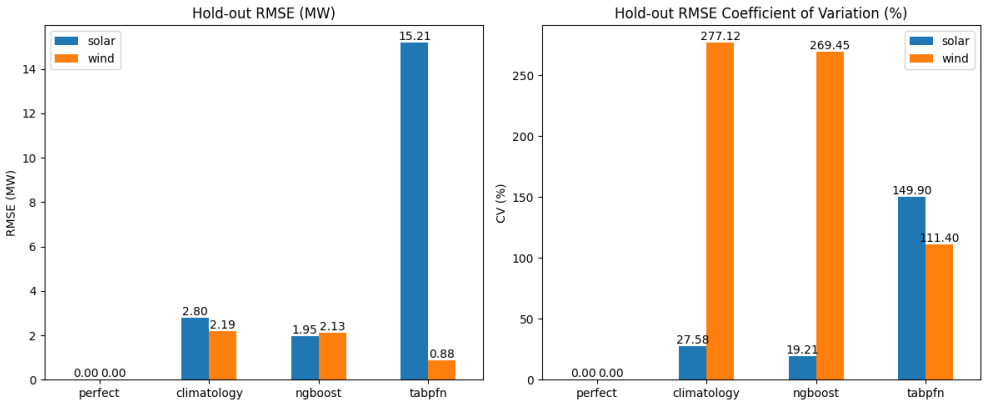

Figure 1: Comparison of Hold-out RMSE (MW) and Coefficient of Variation (CV%) for Solar and Wind Forecasting Models.

The RMSE and coefficient of variation (CV) comparisons in **Figure 1** reveal key differences in forecasting accuracy across the models and resource type. For instance, the Climatology model delivers moderate accuracy: for solar it records an RMSE of 2.80 MW with a CV of 27.6%, whereas for wind the RMSE is 2.19 MW but the CV soars to 277.1%, reflecting wind's greater variability.

NGBoost shows a marked improvement over Climatology for solar, reducing the RMSE to 1.95 MW and the CV to 19.21%, highlighting its ability to capture solar variability more accurately. However, NGBoost's performance for wind is only marginally better than Climatology, indicating persistent challenges in predicting wind power with this model.

TabPFN, on the other hand, shows a contrasting performance. It achieves the lowest RMSE for wind (0.88 MW) and a relatively lower CV of 111.40%, suggesting that TabPFN effectively models wind speed variability. However, its performance on solar predictions is poor, with a significantly high RMSE of 15.21 MW and CV of 149.90%. This suggests that TabPFN struggles to generalize for solar data, likely due to the model's architecture being better suited for capturing temporal patterns typical of wind rather than solar irradiance.

3.2 Grid Fallback

The empirical cumulative distribution function (CDF) plots for solar and wind grid fallback in **Figure 3** shows how each model affects reliance on grid electricity. In the solar CDF, the Climatology model produces the highest fallback (140,000 MWh), indicating frequent reliance on the grid due to inaccurate solar predictions. NGBoost shifts most fallback values down to approximately 135,000 MWh, demonstrating its improved ability to capture solar variability. In contrast, TabPFN performs the worst, with fallback clustered around 125,000 MWh, suggesting that its transformer-based architecture struggles with the rapid fluctuations inherent in solar irradiance.

The wind CDF, the Climatology model again has the highest fallback ($\tilde{2}$20,000 MWh). NGBoost substantially reduces this to around 215,000 MWh, reflecting better wind-power predictions. TabPFN also shows reduced fallback compared to Climatology, with most values around 218,000 MWh, though it slightly underperforms compared to NGBoost.

Overall, NGBoost outperforms Climatology and TabPFN for both solar and wind forecasting, with the most substantial improvement observed in solar predictions. TabPFN performs well for wind but poorly for solar, indicating that its architecture is better suited for capturing temporal patterns typical of wind variability rather than solar irradiance fluctuations.

3.3 Grid Fallback and Demand Met

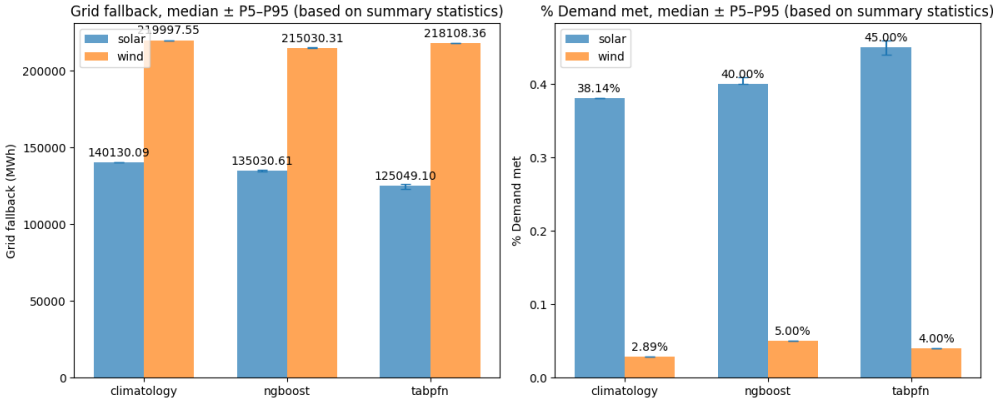

Figure 3: Grid Fallback and Percent Demand Met: The left plot shows the grid fallback, while the right plot shows the proportion of demand met, both expressed as the median ± P5-P95 range based on summary statistics.

In the left panel of Figure 4, we compare median grid fallback volumes and the corresponding percentages of demand met for both solar and wind under each forecasting model. The Climatology model exhibits the highest reliance on the grid, with 140,130 MWh of solar fallback and 219,997 MWh of wind fallback—reflecting its limited ability to anticipate real-time variability. NGBoost markedly reduces this dependency, bringing solar fallback down to 135,030 MWh and wind fallback to 215,030 MWh, which underscores its stronger skill at capturing resource fluctuations. TabPFN achieves the lowest solar shortfall at 125,049 MWh despite its higher overall error, but for wind it only slightly improves on the baseline, with 218,108 MWh of fallback.

When looking at how much demand is met by renewables, both machine-learning models outperform Climatology. NGBoost supplies 40.0 % of solar demand and 5.0% of wind demand, compared to 38.1% and 2.9% under Climatology. TabPFN edges out NGBoost for solar—meeting 45.0% of demand—but delivers only 4.0% for wind. Taken together, these results show that NGBoost provides the most reliable improvements across both resources, while TabPFN excels specifically at solar forecasting and remains less consistent for wind.

3.4 Analysis of Cost Distribution

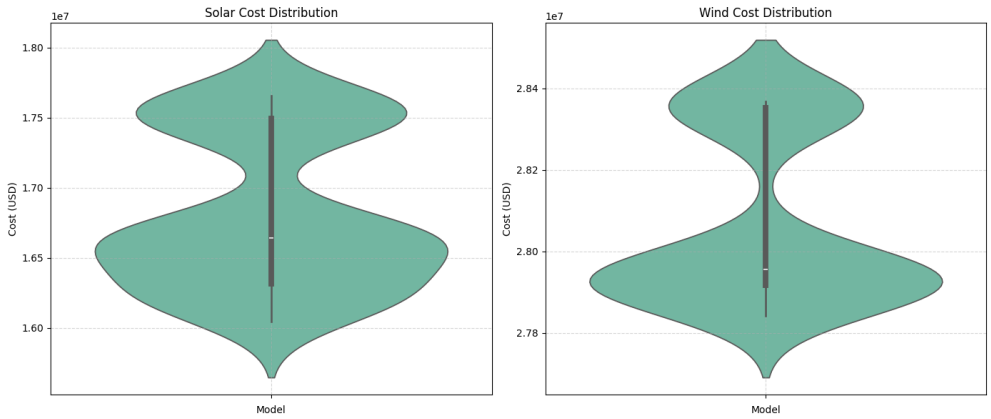

Figure 4: Violin plots of cost distribution (USD) for solar (left) and wind (right) forecasts. The figures illustrate how forecast accuracy impacts operation costs, highlighting the variability and central tendency for each energy source

The solar cost distribution (left plot) has a bimodal shape, indicating two main cost clusters, with the median around 1.70 × 10 USD. The distribution spans from 1.60 × 10 to 1.80 × 10 USD, showing significant variability. The narrow central waist suggests more consistent costs near the median, but the wider tails indicate that forecast errors can result in higher or lower operational costs. This reflects the greater unpredictability of solar power generation, which can lead to fluctuating expenses.

The wind cost distribution (right plot) also shows a bimodal pattern, but with a narrower central range. The median cost is approximately 2.80 × 10 USD, with a range between 2.78 × 10 and 2.84 × 10 USD. This more compact distribution indicates lower variability compared to solar, suggesting that wind forecasts are more stable. However, the bimodal peaks still reflect the impact of forecast errors, though to a lesser extent. Overall, solar forecasting shows greater financial uncertainty, while wind forecasting yields more predictable costs.

4 Discussion

The results of this study demonstrate significant differences in forecasting accuracy between the models for both solar and wind energy. The primary goal of this project was to optimize renewable-powered data center operations by minimizing grid fallback, reducing carbon emissions, and maintaining cost efficiency. Based on the analysis, it is evident that model selection plays a crucial role in achieving these objectives.

4.1 Interpretation of Results

In my analysis, NGBoost demonstrated the best performance for solar forecasting. It achieved substantially lower RMSE and coefficient of variation than both the Climatology and TabPFN models, which translated into notably fewer hours of grid dependency. This increased precision is especially valuable in solar-rich regions such as Yuma, Arizona, where better alignment between predicted and actual solar output directly reduces reliance on backup generation. In contrast, TabPFN's transformer-based architecture struggled to capture rapid, short-term fluctuations in solar irradiance, resulting in higher forecast errors and increased grid fallback.

For wind forecasting, TabPFN outperformed both NGBoost and Climatology, delivering the lowest RMSE and CV and reducing grid fallback more effectively. Its strength in modeling temporal consistency makes it ideally suited to sites like Mount Storm, West Virginia, where wind patterns follow clear, regular cycles. Although NGBoost provided modest improvements

over Climatology for wind, it did not match the consistency and reliability of TabPFN's predictions.

My cost-distribution analysis further highlights the resource-specific nature of forecast error impacts. Solar forecasting errors introduce far greater financial volatility than wind, as small deviations in irradiance can lead to large swings in grid purchases. NGBoost helps contain this variability for solar, whereas TabPFN yields the most stable cost outcomes for wind. These findings illustrate the importance of tailoring model choice to both resource type and local climate conditions in order to manage financial risk effectively.

Based on these insights, I recommend using NGBoost for solar forecasts and TabPFN for wind forecasts. In mixed-resource data centers, a hybrid strategy that deploys NGBoost for solar and TabPFN for wind will leverage each model's strengths and minimize overall forecast error. To further enhance operational resilience, integrating a battery energy storage system with an adaptive dispatch algorithm can buffer remaining forecast inaccuracies, smooth renewable output, and further reduce dependency on grid power.

4.2 Limitations

This study has several limitations. First, my evaluation relies on hourly data from only two geographic sites, which may not capture sub-hourly variability or regional climatic differences. Second, the dispatch simulation employs a greedy algorithm and fixed cost parameters, omitting factors such as dynamic electricity pricing, maintenance outages, and ancillary-service markets. Third, I compare only NGBoost and TabPFN against simple baselines; evaluating additional machine-learning techniques, such as ensemble tree algorithms or hybrid deep-learning approaches, could reveal further improvements. Fourth, assumptions regarding solar panel efficiency, turbine performance, and other input parameters may not reflect real-world variability. Fifth, my Gaussian-error assumptions for NGBoost and static transformer pretraining for TabPFN may not hold under extreme weather events or non-stationary climate trends. Sixth, the study's applicability is limited by its hypothetical data center setup, which may not scale to complex, real-world energy infrastructures. Finally, my focus on static grid fallback cost estimation overlooks the dynamic nature of electricity pricing, which can vary significantly across regions and timeframes.

Addressing these limitations by expanding geographic scope, incorporating higher-resolution and more diverse datasets, modeling dynamic pricing and operational constraints, and testing a broader range of forecasting and dispatch strategies will enhance the robustness and practical relevance of these findings.

References

Penn State EMSC 297. Solar pv performance: How to calculate performance ratio. Pennsylvania State University, 2025. https://www.e-education.psu.edu/emsc297/node/649.

ASCEE. International journal of research in community services (ijrcs). ASCEE, 2025. https://pubs2.ascee.org/index.php/ijrcs.

Joint Legislative Audit and Review Commission (JLARC). Virginia data center study. Commonwealth of Virginia, 2024. https://jlarc.virginia.gov/pdfs/presentations/JLARC%20Virginia%20Data%20Center%20Study_FINAL_12-09-2024.pdf.

National Climatic Data Center. Sunniest u.s. cities, 2024. https://www.ncei.noaa.gov.

E3. Load growth is here to stay, but are data centers? E3 White Paper, 2024. https://www.ethree.com/wp-content/uploads/2024/07/E3-White-Paper-2024-Load-Growth-Is-Here-to-Stay-but-Are-Data-Centers-2.pdf.

U.S. Energy Information Administration (EIA). Electricity monthly update. U.S. Energy Information Administration. https://www.eia.gov/electricity/monthly/epm_table_grapher.php?t=epmt_5_3.

U.S. Energy Information Administration (EIA). Wholesale electricity markets. U.S. Department of Energy, 2025. https://www.eia.gov/electricity/monthly/update/wholesale-markets.php.

Dominion Energy. Mount storm wind farm fact sheet, 2024. https://www.dominionenergy.com.

Uptime Institute. Global data center survey 2024. Uptime Intelligence Report, 2024. https://uptimeinstitute.com/.

International Renewable Energy Agency (IRENA). Renewable power generation costs in 2023. International Renewable Energy Agency, 2024. https://www.irena.org/Publications/2024/Sep/Renewable-Power-Generation-Costs-in-2023.

Mdpi. Renewable energy modeling techniques. *Energies*, 12(4):646–657, 2019. https://www.mdpi.com/1996-1073/12/4/646.

National Renewable Energy Laboratory (NREL). Windexchange: Maps and data. U.S. Department of Energy, a. https://windexchange.energy.gov/maps-data.

National Renewable Energy Laboratory (NREL). Land-use requirements for wind turbines. U.S. Department of Energy, b. https://www.nrel.gov/.

National Renewable Energy Laboratory (NREL). Wind energy in west virginia (fact sheet). Technical Report NREL/TP-6A20-70738, U.S. Department of Energy, 2018. https://www.nrel.gov/docs/fy18osti/70738.pdf.

National Renewable Energy Laboratory (NREL). Energy storage futures study. U.S. Department of Energy, 2021a. https://www.energy.gov/sites/default/files/2021/06/f37/2021-Storage-Futures.pdf.

National Renewable Energy Laboratory (NREL). National solar radiation data base (nsrdb). U.S. Department of Energy, 2021b. https://nsrdb.nrel.gov/.

Solar Energy Industries Association (SEIA). Utility-scale solar power overview. Solar Energy Industries Association. https://www.seia.org/.

First Solar. Utility-scale pv power plants. First Solar. https://www.firstsolar.com/.

Maysun Solar. Performance ratio: Do you know how to calculate it? Maysun Solar Blog, 2025. https://www.maysunsolar.com/blog-performance-ratio-do-you-know-how-to-calculate-it.

Vestas. V100-2.0 mw specs. GE Renewable Energy Turbines. https://www.vestas.com/.